Nationaal Lucht- en Ruimtevaartlaboratorium
National Aerospace Laboratory NLR

NLR-TP-2002-226

Determination of absolute levels from phased array measurements using spatial source coherence

S. Oerlemans and P. Sijtsma

Nationaal Lucht- en Ruimtevaartlaboratorium
National Aerospace Laboratory NLR

NLR-TP-2002-226

Determination of absolute levels from phased array measurements using spatial source coherence

S. Oerlemans and P. Sijtsma

The contents of this report have been initially prepared for publication as AIAA paper 2002-2464 in the proceedings of the 8th AIAA/CEAS Aeroacoustics Conference, Breckenridge, Colorado, 17-19 June 2002.

Customer:	National Aerospace Laboratory NLR
Working Plan number:	A.2.C.1
Owner:	National Aerospace Laboratory NLR
Division:	Fluid Dynamics
Distribution:	Unlimited
Classification title:	Unclassified
	May 2002

Contents

11 Figures

(13 pages in total)

DETERMINATION OF ABSOLUTE LEVELS FROM PHASED ARRAY MEASUREMENTS USING SPATIAL SOURCE COHERENCE

Stefan Oerlemans*, Pieter Sijtsma¶
National Aerospace Laboratory NLR, PO Box 153, 8300 AD Emmeloord, The Netherlands

The phased array technique is a valuable tool in acoustic testing for its capability to distinguish between different source locations. However, the interpretation of phased array measurements is still difficult due to the simultaneous occurrence of several effects: the size and level of a spot in a conventional acoustic 'source plot' may be affected by a combination of (1) the limited resolution of the array (2) coherence loss during propagation to the array (3) the spatial extent of the source region. This ambiguity complicates the determination of absolute source levels from phased array measurements. The current paper addresses this problem for a noise source that is extended mainly in one direction, i.e. trailing-edge noise. Simulations are done for a line source, and the influence of array resolution and source coherence length on the array output is investigated. Furthermore, an array processing technique is presented which determines the coherence level between different sources in the scan plane. As a first application, the technique is used to identify mirror sources in a closed wind tunnel. The new method is then applied to trailing-edge noise measurements in NLR's Small Anechoic Wind Tunnel, in order to estimate the spanwise coherence length. In conjunction with the simulations this enables an improved determination of absolute trailing-edge noise from phased array measurements.

1 INTRODUCTION

In the last decade, phased arrays have been increasingly used for acoustic testing of both stationary[1,2] and, more recently, moving sound sources[3,4]. The main advantage of this technique with respect to single microphone measurements is that contributions coming from different source directions can be separated from each other and from background noise. In this way, acoustic measurements are possible in situations with high background noise levels (e.g. closed test section wind tunnels[5,6,7]), and different noise sources can be distinguished. Thus, the acoustic array technique has proven its ability to locate sound sources. However, the problem of determining the absolute levels of the located sources is still a subject under investigation.

Due to the presence of several (background) noise sources, often the sound levels at the individual microphones cannot be used to determine absolute levels or spectra for the different sources. As a result, one has to characterize the different noise sources using the output of the phased array. For incoherent, separate monopole sources the absolute sound level corresponds to the peak level in the acoustic 'source plot'. However, in practice the interpretation of phased array results is difficult due to the simultaneous occurrence of several effects: the size and level of a spot in a conventional acoustic 'source plot' may be affected by a combination of (1) the limited resolution of the array (2) coherence loss during propagation to the array (3) the spatial extent of the source region. This ambiguity complicates the determination of absolute source levels from phased array measurements.

In the last few years, a number of studies have addressed this problem by integration methods[8,9]. Brooks *et al.*[8] defined an integration area around the source region and calculated a frequency dependent array calibration function, assuming a source distribution of uncorrelated monopoles. The method was applied to simulations of a line source and to measurements of a calibrator source and flap side-edge noise. The measurements were done with arrays of different aperture. It was found that absolute spectra of the different sources could well be recovered from the phased array results, as long as the sources were not too close to the boundary of the integration box. Even effects of coherence loss (due to scattering by jet shear layer turbulence), which typically yield a lower but broader peak and which depend on array size, did not reduce the quality of the results significantly: integrated levels generally

* Research Engineer, Aeroacoustics Department
e-mail: stefan@nlr.nl
¶ Research Engineer, Aeroacoustics Department
e-mail: sijtsma@nlr.nl

agreed within 1.5 dB for different arrays and Mach numbers. However, when the array processing algorithm was applied after removal of the main diagonal from the cross-spectral density matrix, which is often done in situations with low signal-to-noise ratio, the integration technique was less reliable. This may be caused by the fact that the cross-spectral density matrix is no longer positive-definite, which can lead to non-physical results in the source plot (negative autopowers). As a result the diagonal-removal technique is not well suited for acoustic energy calculations based on integrated scan levels.

Horne *et al.*[9] investigated the effect of source coherence of two monopole sources on the response of a phased acoustic array. It was found that both peak and integrated response levels varied significantly as a function of phase and coherence level between the two sources. Ostertag *et al.*[10] investigated trailing-edge noise from a flat plate and determined both theoretically and experimentally an array transfer function relating the levels in the acoustic source plots to absolute sound levels in the farfield. Good agreement between the measured and predicted array calibration function was found.

The motivation for the current study is the interpretation of trailing-edge noise measurements of 2D airfoil sections (chord 0.2 m) in NLR's Small Anechoic Wind Tunnel (see Figure 1). The set-up for these measurements is described in more detail elsewhere[11]; the array processing was done using conventional beamforming[12]. Although the trailing-edge noise source was clearly visible in the acoustic source plots (Figure 2*a*), the sound levels at the array microphones could not be used to determine the trailing-edge noise spectra, due to relatively high background noise levels. Simply subtracting a background noise measurement (without model in the test section) from the measured data is not reliable due to the presence of extraneous noise sources at the model/side-plate junctions (caused by the turbulent boundary layer on the side-plates) and possibly other model-induced noise. The high background noise level becomes apparent when diagonal-removal processing is *not* applied (Figure 2*b*). As a result of this 'contamination' of the sound levels at the array microphones, determination of absolute trailing-edge noise spectra should be done on the basis of the phased array results.

The integration technique mentioned above[8] cannot be used here for a number of reasons. First, the integration technique assumes a distribution of uncorrelated sources, while in reality trailing-edge noise has a non-zero spanwise correlation length. Second, the integration technique works well only when no diagonal-removal processing is used. However, for the present case these results are contaminated by background noise and can therefore not be used for the integration technique. For that reason this paper describes an alternative method to determine absolute trailing-edge noise spectra from phased array measurements.

In Section 2, the influence of array resolution and source coherence is investigated by performing simulations for a line source with varying coherence length. From these simulations the maximum level in the source plot can be related to the absolute sound level at the array, as a function of source coherence length. Section 3 describes an array processing method by which the coherence between different sources in the scan plane can be determined. As a first check this technique is used to identify mirror sources in a closed wind tunnel. In Section 4 the new method is applied to the trailing-edge noise measurements, in order to estimate the spanwise correlation length. In conjunction with the simulations described in Section 2 the absolute trailing-edge noise spectrum is determined and compared to predictions. Section 5 summarizes the conclusions.

2 SIMULATIONS OF LINE SOURCE

Numerical model

Brooks *et al.*[8] used an analytical model to calculate the response of a phased array to a line source. This analytical model is not suited for the present investigation for two reasons. First, the analytical line source is a distribution of uncorrelated monopoles, while one purpose of the present study is to investigate the influence of coherence length on the array output. Second, the analytical model assumes that the length of the line source is much smaller than the distance to the array, which is not the case in the present study. Therefore, here the trailing-edge noise source was simulated by an array of equidistant monopole sources of uniform strength. As a consequence, the directivity in planes perpendicular to the axis of the line source is uniform. Due to the quadrupole character of the aeroacoustic sources and the diffraction effect of the wing, in reality trailing-edge noise will exhibit a much more complex directivity. However, as long as we limit ourselves to the immission on a microphone array with a limited solid angle the use of the monopole approximation will be sufficient.

The spanwise coherence length was varied by defining groups of coherent (in-phase) monopoles. The cross power matrix for this source distribution was generated by retaining the cross terms between coherent monopoles and eliminating the cross terms between incoherent monopoles, which is equivalent to an infinite number of averages. From the cross power matrix acoustic source plots were calculated

using conventional beamforming with a scan resolution of 1 cm in both directions. The levels in the source plots are reconstructed Sound Power Levels; the dynamic range in all source plots is 15 dB.

The set-up for the simulations was chosen similar to the experimental set-up, for later comparison purposes. The array position and layout, and the frequency resolution (40 Hz) were identical to the experiments. Although in the experiments the model was mounted between two (acoustically lined) side-plates at a distance of 0.5 m, in the simulations the length of the line source was taken to be 0.6 m to account for reflections from the parts of the trailing-edge close to the side-plates. For the regions further away from the (lined) side-plates it was shown in a previous study that reflections do not influence the scan levels[11]. The length of 0.6 m was chosen on the basis of source plots with larger scan planes than shown in Figure 2, and was taken to be independent of frequency for simplicity. The number of monopoles used to represent the 0.6 m line source was chosen to be 64 in order to enable formation of various coherent 'group sizes'. Numerical experimentation with a larger or smaller number of monopoles showed practically identical results (differences smaller than 0.2 dB), as long as the distance between the monopoles was small enough with respect to the main lobe width.

Array calibration function

The numerical results to be shown subsequently will be used to relate the array output to the immission (from the line source) on the array, where the immission is defined as the average sound pressure level at the array microphones. For this purpose the *array calibration function (ACF)* is defined that will be applied throughout this paper to both simulations and experimental results.

Due to the background noise contamination of the experimental source plots without diagonal-removal processing (see Figure 2*b*), the source plots *with* diagonal-removal processing will be used for the ACF. As mentioned in the introduction, the integration method[8] does not work very well for these plots. Therefore, the *peak* level in the acoustic source plots will be used to characterize the trailing-edge noise level. The use of peak levels may give problems in cases where coherence loss (due to propagation of the sound through the shear layer) is present. However, for the present configuration it was shown before[11] that these effects are small up to 8 kHz. Furthermore, the absence of coherence loss was verified by processing the experimental data with a reduced array size (in streamwise direction), which gave broader peaks but practically identical peak levels. Finally, comparison with numerical results for the line source shows no indication of an increased peak width in the experimental case (see below).

The trailing-edge peak levels in the source plots were averaged in spanwise direction. In order to avoid disturbance from the extraneous noise sources at the model-endplate junctions (Figure 2), only the part of the span in the middle of the test section (10 cm) was used for this average. In conclusion, the ACF is defined as the average trailing-edge (or line source) peak level in the acoustic source plot minus the average immission (from the line source) on the array microphones (in dB's).

Numerical results

From literature[13], the expected spanwise correlation length beneath an attached turbulent boundary layer can be estimated to be quite small, i.e. $U_c /(2\pi \gamma_3 f)$, where $U_c \approx 0.7 \cdot U_D$ is the eddy convection velocity, $\gamma_3 \approx 0.8$ is a dimensionless parameter, and f is the frequency. However, in order to obtain insight in the effect of a varying coherence length, simulations were done for coherence lengths ranging from less than a centimeter (i.e. an uncorrelated line source) to the complete source length (60 cm). As an example, Figure 3 and Figure 4 show acoustic source plots in 1/3-octave bands for the uncorrelated line source and for a line source consisting of four groups of sixteen coherent monopoles (coherence length 15 cm). The plots for the uncorrelated line source (with diagonal-removal processing) show a good qualitative agreement with the corresponding experimental plots in Figure 2*a*, except of course for the extraneous sources at the model/side-plate junctions. The simulated plots without diagonal-removal processing show larger differences with the experimental plots, indicating the presence of background noise in the main diagonal of the experimental cross power matrix. Simulations with coherence lengths up to 7.5 cm (not shown) showed practically identical source plots. The plots for the line source with a coherence length of 15 cm (Figure 4) show differences at the edges, but look quite similar to the incoherent case in the middle.

In order to interpret the measured source plots, we would like to relate the levels in the simulated source plot to the absolute sound levels at the array. For this purpose, the array calibration function (see above for definition) is plotted in Figure 5 as a function of frequency, for a number of coherence lengths. As a reference the line relating the peak level of a monopole source to the array immission is also shown. The line for the uncorrelated line source shows a frequency dependent calibration factor with a range of about 8 dB between 1 and 8 kHz. This behaviour is in good agreement with the curve obtained by Brooks *et al.*[8], although in the present case their assumption that the

source length is much smaller than the distance to the array is not satisfied (both are 0.6 m). The ACF is also similar to the calibration function found by Ostertag *et al.*[10] for similar conditions. The shape of the curve can be qualitatively understood from the fact that the scan levels for a group of incoherent sources are equal to the sum of the scan levels from the individual sources. Thus, for low frequencies (i.e. low resolution), more 'double-counting' occurs resulting in a high value of the ACF. Therefore, although the dependence on the different parameters was not systematically investigated, the ACF for an uncorrelated line source is expected to depend only on the array resolution (i.e. frequency, array size, and distance to the array) and on the length of the line source.

For correlated sources the above reasoning does not hold and the behaviour of the ACF is more complicated. The dependence of the ACF on the coherence length is shown in Figure 5. It can be seen that for higher frequencies differences with the uncorrelated line source occur up to almost 4 dB. For lower frequencies the differences are smaller, since, up to some coherence length, the array simply 'sees' a group of neighboring coherent sources as one source, due to the limited array resolution. Note that for the coherence length of 15 cm the ACF changes when a different position of the coherent regions is chosen (instead of four times 16 coherent monopoles a distribution of 8,16,16,16,8 was chosen, so that one coherent region is located in the center of the test section). For coherence lengths of 7.5 cm and lower these differences as a function of the position of the coherent regions were negligible. It may be possible that the differences in the ACF as a function of coherence length are smaller when an integration method is used instead of peak levels. However, for the present study this was not possible due to the relatively high background noise levels in the experiments (see Section 1).

In conclusion, the only unknown required to relate the peak levels in the acoustic source plots to absolute source spectra is the coherence length. From Figure 5 it can be concluded that if no knowledge is available on the coherence length, the absolute sound level of a line source can in principle not be determined from the acoustic source plots: in the present case errors of the order of 4 dB could be induced by misinterpretation of the data. Therefore, in the next section a method will be presented that enables the estimation of coherence lengths on the basis of the phased array results.

3 DETERMINATION OF SOURCE COHERENCE

As mentioned in the previous section, information on the coherence length of the line source is needed to relate the peak levels in the acoustic source plot to absolute sound levels. The coherence length can be estimated by calculating the coherence between different scan points in the acoustic source plot. As already suggested by Horne *et al.*[9], this coherence can be obtained by a modification of the beamforming algorithm. In conventional beamforming (without diagonal-removal processing) the array output for a given scan location is

$$\frac{\mathbf{e}^{*}\mathbf{C}\,\mathbf{e}}{\left(\mathbf{e}^{*}\mathbf{e}\right)^{2}} \tag{1}$$

where * denotes the complex conjugate, **e** is the steering vector corresponding to the scan point and **C** is the averaged cross power matrix. For the determination of the coherence level between two scan points we use

$$\frac{\left|\mathbf{e}^{*}\mathbf{C}\,\mathbf{d}\right|^{2}}{(\mathbf{e}^{*}\mathbf{C}\,\mathbf{e})(\mathbf{d}^{*}\mathbf{C}\,\mathbf{d})} \tag{2}$$

where **d** is the steering vector for the second scan point. Note that the denominator is proportional to the product of the array outputs in both scan points. In order to obtain physical values for the coherence, equation (2) should be applied to the full cross power matrix, i.e. without diagonal-removal processing.

The method is first applied to simulations with two incoherent monopole sources, using the same array layout as before. As an example typical results of these simulations are given in Figure 6. Besides the conventional source plots also 'coherence plots' are presented, which show the coherence of all scan points with respect to one reference point (in this case the reference point is the right-hand source). At 4 kHz the array resolution is sufficient to separate the two sources, and as expected the coherence plot shows zero coherence at the position of the second source. The high coherence levels around the two sources are due to the fact that sidelobes, although they have a low level in the conventional source plot, are fully coherent with the original source. This indicates that the coherence plots may be used to identify sidelobes in acoustic source plots. It will be shown later that in experimental coherence plots these sidelobes can be less prominent due to the presence of background noise. At 1250 Hz, it can be seen that although the resolution is so low that the two sources cannot be distinguished in the conventional source plot, the coherence plot clearly shows a transition. Thus, from the coherence plot the presence of two, incoherent sources can be determined. If the sources are coherent (irrespective of their phase difference), the coherence level is equal to one for all scan points.

Next, the coherence method was applied to identify mirror sources in array measurements of a calibration source in a closed wind tunnel test section (DNW-Low Speed Wind Tunnel). Figure 7 shows the

experimental set-up and the location of the calibration source and its mirror source. The 96 microphone array was flush-mounted in the tunnel wall.

The experimental acoustic source plots (without flow) clearly show two sources (Figure 8*a*), and the coherence plots confirm the coherence between the original and mirror source (Figure 8*b*). Furthermore, the coherence plots clearly show the sidelobes of the real source, especially at higher frequencies. The coherence level does not equal one for all scan points (as would be the case for a single source in an anechoic environment) because in a given FFT time block reflections are present from previous time blocks, which are incoherent with the signal in the present time block. This was confirmed by calculating coherence plots with a larger block size (so that more reflections are present in one block), which showed higher coherence levels (Figure 8*c*). In case of flow (not shown) the mirror source was much less clear in the coherence plot, due to the high background noise levels from the wall boundary layer. This could be anticipated from the fact that the sources were hardly visible in the acoustic source plot without diagonal-removal processing. A solution to this may be the application of equation (2) *with* diagonal-removal processing, but this can lead to non-physical values of the coherence level.

In the next section, the coherence method will be applied to estimate the spanwise coherence length in the trailing-edge noise measurements discussed before.

4 TRAILING-EDGE NOISE MEASUREMENTS

In Section 2 it was shown that the ACF, which relates the peak levels in the acoustic source plots to absolute sound levels at the array microphones, depends on the coherence length of the line source. In Section 3 a method was developed which enables the determination of the coherence level between different scan points. In this section the coherence method will be applied to the trailing-edge noise measurements, in order to estimate the spanwise coherence length. Using the ACF the absolute trailing-edge noise spectrum can then be determined. In this section only frequency bands of 2 kHz and higher will be considered, since for lower frequencies the wavelength is larger than the airfoil chord so that the noise source cannot be modeled as a line source located at the trailing-edge.

Figure 9*a* shows the coherence plots for the trailing-edge noise measurements (see also Figure 2). These plots show that the coherent region is limited to some length of the trailing-edge, depending on frequency. In order to interpret these results, and to separate array resolution effects from real coherence, Figure 9*b* shows simulated coherence plots for the uncorrelated line source (see also Figure 3). It can be seen that the shape of the coherent spots is quite different from the experimental plots. This can be understood if we realize that the coherence plots are based on the full cross power matrix (without diagonal-removal): in the simulations, the sidelobes are fully coherent with the main lobe. In the experimental data however, at the sidelobes the denominator of equation (2) is dominated by noise (compare Figure 2*b* to Figure 3*b*). Thus, the outcome of equation (2) at these locations is much less than without noise.

Therefore, in the simulations uncorrelated background noise was added to the main diagonal in the cross power matrix. For this purpose first the level of the line source at the trailing-edge was taken such that the peak level in the source plot with diagonal-removal processing (as defined for the ACF, see Section 2) was equal to the experimental value. Then the level of the background noise was chosen such that the average level in the simulated source plot *without* diagonal elimination was equal to the experimental value (as a function of frequency). The results for an uncorrelated line source are shown in Figure 10*a* and *b*. It can be observed that after the addition of noise both the source plots without diagonal-removal processing and the coherence plots look much more like the experimental ones. (The source plot *with* diagonal-removal processing does not change after noise addition and is therefore identical to Figure 3*a*.)

The simulated coherence plot for a line source (with noise) with a coherence length of 15 cm (five groups consisting of 8,16,16,16,8 coherent monopoles) is shown in Figure 10*c*. Comparison of Figure 10*b* and 10*c* shows that the differences between the two coherence plots are quite small due to the limited array resolution in spanwise direction. For coherence lengths of 7.5 cm or smaller the simulated coherence plots were practically identical to those for the uncorrelated line source. Thus, for these measurements the coherence plots can only provide an upper limit for the coherence length.

As mentioned in Section 2, on the basis of the literature[13] the expected spanwise coherence length for the current conditions is less than 0.5 cm for 2 kHz and higher. In conjunction with the coherence plots it therefore seems justified to assume that the coherence length is less than 4 cm for all frequencies, which means that the ACF for the uncorrelated line source (see Figure 5) can be used to relate the peak levels in the acoustic source plots to absolute spectra. Figure 11 shows the peak levels together with the reconstructed trailing-edge noise spectrum, which was obtained by subtracting the ACF for the uncorrelated line source from the peak

level. The reconstructed spectrum is compared to the predicted trailing-edge noise spectrum for the current airfoil shape and test conditions[14]. As can be seen in Figure 11 good agreement is found, indicating that a realistic spectral shape and level is obtained.

5 CONCLUSIONS

In acoustic testing often single-microphone measurements are not sufficient to determine source levels, due to the presence of several (background) noise sources. Instead, the phased array technique can be applied to distinguish noise coming from different directions. The determination of absolute noise levels from phased array results is however still complicated due to the simultaneous occurrence of a number of effects. In the current paper this problem is addressed for trailing-edge noise.

First, simulations are done for a line source with variable coherence length. It is shown that a frequency dependent calibration function should be applied to the peak levels in the acoustic source plot in order to obtain absolute sound levels. This calibration function is found to depend on the coherence length of the line source.

Next, a method is presented which enables determination of the coherence level between different scan points in the acoustic source plot. The technique is applied in simulations, which shows that even when the resolution is low, incoherent sources can be identified in so called 'coherence plots'. Furthermore, the method was successfully applied to identify mirror sources in a closed test section wind tunnel. This new array processing method offers potential for the determination of the coherence length of distributed sources (such as slat noise or jet noise) and for the identification of sidelobes and mirror sources (e.g. in closed wind tunnels or landing gear below a wing).

Finally, the coherence method is applied to trailing-edge noise measurements, in order to estimate the spanwise coherence length. The background noise level in the experiments is determined on the basis of the acoustic source plots and coherence plots. Using the array calibration function for an uncorrelated line source, the trailing-edge noise spectrum is determined from the peak levels in the acoustic source plots, and good agreement with the predicted spectrum is found.

ACKNOWLEDGMENTS

The trailing-edge noise measurements in NLR's Small Anechoic Wind Tunnel were performed in the framework of the European project DATA ('Design and Testing of Acoustically Optimized Airfoils for Wind Turbines'). The measurements on the calibration source in DNW-LST were performed under a contract awarded by the German-Dutch Wind Tunnels DNW. S. Oerlemans would like to thank A. Hirschberg and M.E.H. Van Dongen from Eindhoven University of Technology for the fruitful discussions.

REFERENCES

[1] Meadows, K.R., Brooks, T.F., Humphreys, W.M., Hunter, W.W., and Gerhold, C.H.: 'Aeroacoustic measurements of a wing-flap configuration', AIAA paper 97-1595, 1997.

[2] Piet, J.F., and Elias, G.: 'Airframe noise localization using a microphone array', AIAA paper 97-1643, 1997.

[3] Michel, U. Barsikow, B., Helbig, J., Hellmig, M., and Schüttpelz, M.: 'Flyover noise measurements on landing aircraft with a microphone array', AIAA paper 98-2336, 1998.

[4] Sijtsma, P., Oerlemans, S., and Holthusen, H.: 'Location of rotating noise sources by phased array measurements', AIAA paper 2001-2167, NLR-TP-2001-135, 2001.

[5] Sijtsma, P. and Holthusen, H.: 'Source location by phased array measurements in closed wind tunnel test sections', AIAA paper 99-1814, NLR-TP-99-108, 1999.

[6] Storms, B.L., Hayes, J.A., Moriarty, P.J., and Ross, J.C.: 'Aeroacoustic measurements of slat noise on a three-dimensional high-lift system', AIAA paper 99-1957, 1999.

[7] van der Wal, H.M.M. and Sijtsma, P.: 'Flap noise measurements in a closed wind tunnel with a phased array', AIAA paper 2001-2170, NLR-TP-2001-632, 2001.

[8] Brooks, T.F. and Humphreys, W.M.: 'Effect of directional array size on the measurement of airframe noise components', AIAA paper 99-1958, 1999.

[9] Horne, C., Hayes, J.A., Jaeger, S.M., and Jovic, S.: 'Effects of distributed source coherence on the response of phased arrays', AIAA paper 2000-1935, 2000.

[10] Ostertag, J.S.D., Guidati, S., Guidati, G., Wagner, S., Wilde, A, and Kalitzin, N: 'Prediction and measurement of airframe noise on a generic body', AIAA paper 2000-2063, 2000.

[11] Oerlemans, S. and Sijtsma, P.: 'Effect of wind tunnel side-plates on airframe noise measurements with phased arrays', AIAA paper 2000-1938, NLR-TP-2000-169, 2000.

[12] Johnson, D.H. and Dudgeon, D.E.: 'Array Signal Processing', Prentice Hall, 1993.

[13] Blake, W.K.: 'Mechanics of flow-induced sound and vibration', Academic Press, 1986.

[14] Hoffmans, W., Golliard, J., van Lier, L., and Parchen, R.: 'Prediction of turbulent boundary layer trailing-edge noise based on measured and/or computed boundary-layer properties', Proceedings of the 7th International Congress on Sound and Vibration, July 2000.

FIGURES

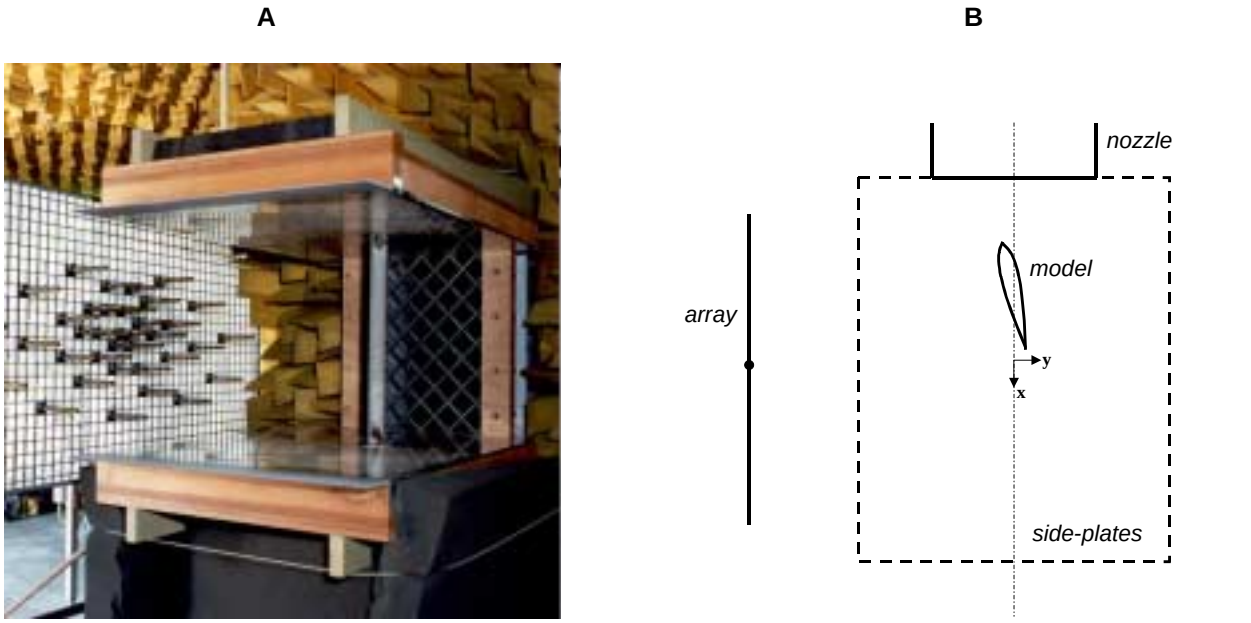

Figure 1: (A) Test set-up in NLR's Small Anechoic Wind Tunnel, with lined side-plates and a sparse array. During the trailing-edge noise measurements, the turbulence grid in the nozzle was not present. (B) Top view.

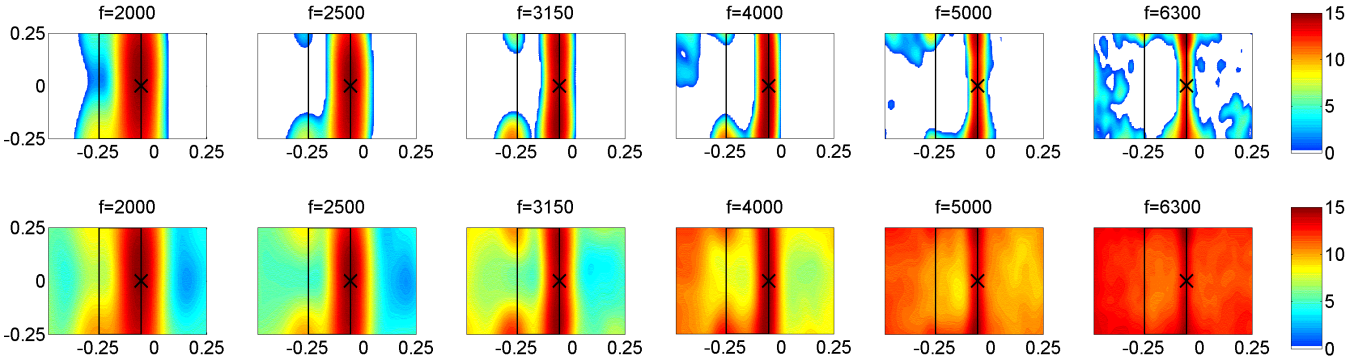

Figure 2: Phased array measurement of 2D airfoil section (M=0.22): (A) Acoustic source plot with diagonal-removal processing. (B) Acoustic source plot without diagonal-removal processing. The airfoil leading- and trailing-edge are indicated in the source plots. The dynamic range is 15 dB.

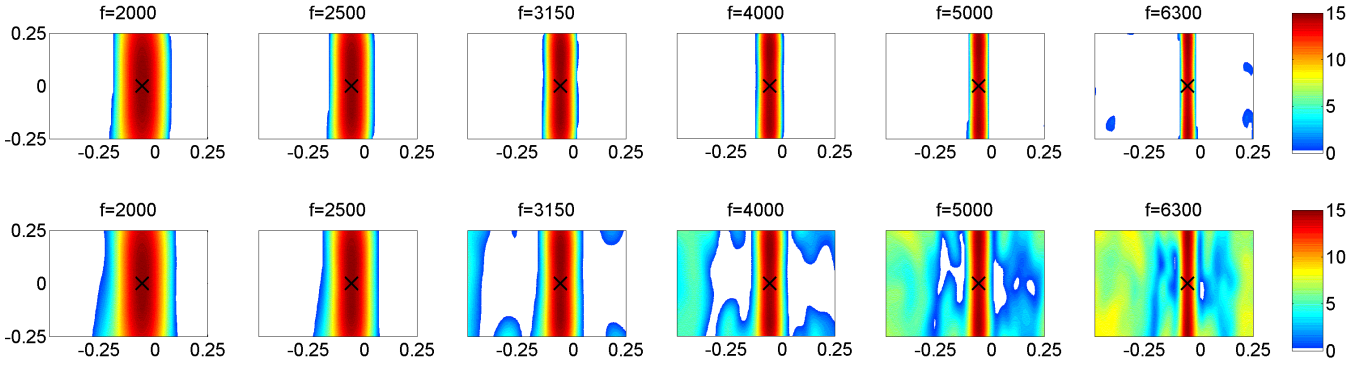

Figure 3: Simulated acoustic source plots for uncorrelated line source: (A) With diagonal-removal processing. (B) Without diagonal-removal processing.

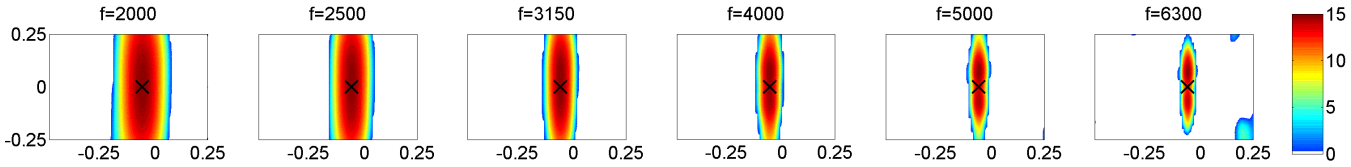

Figure 4: Simulated acoustic source plots for line source with coherence length of 15 cm (with diagonal-removal processing).

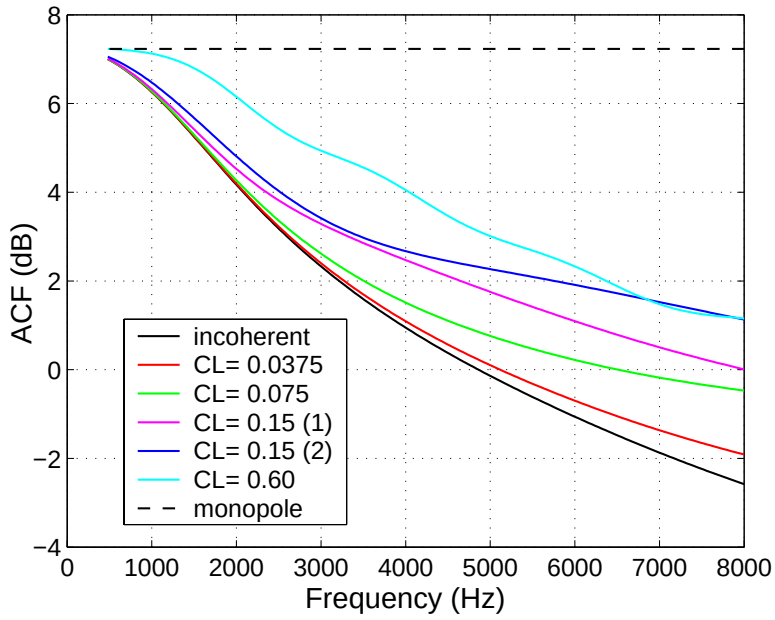

Figure 5: Array calibration function (ACF) for a line source, for different coherence lengths (CL). The array calibration function is defined in Section 2. As a reference the line relating the peak level of a monopole source to the array immission is also shown ('monopole').

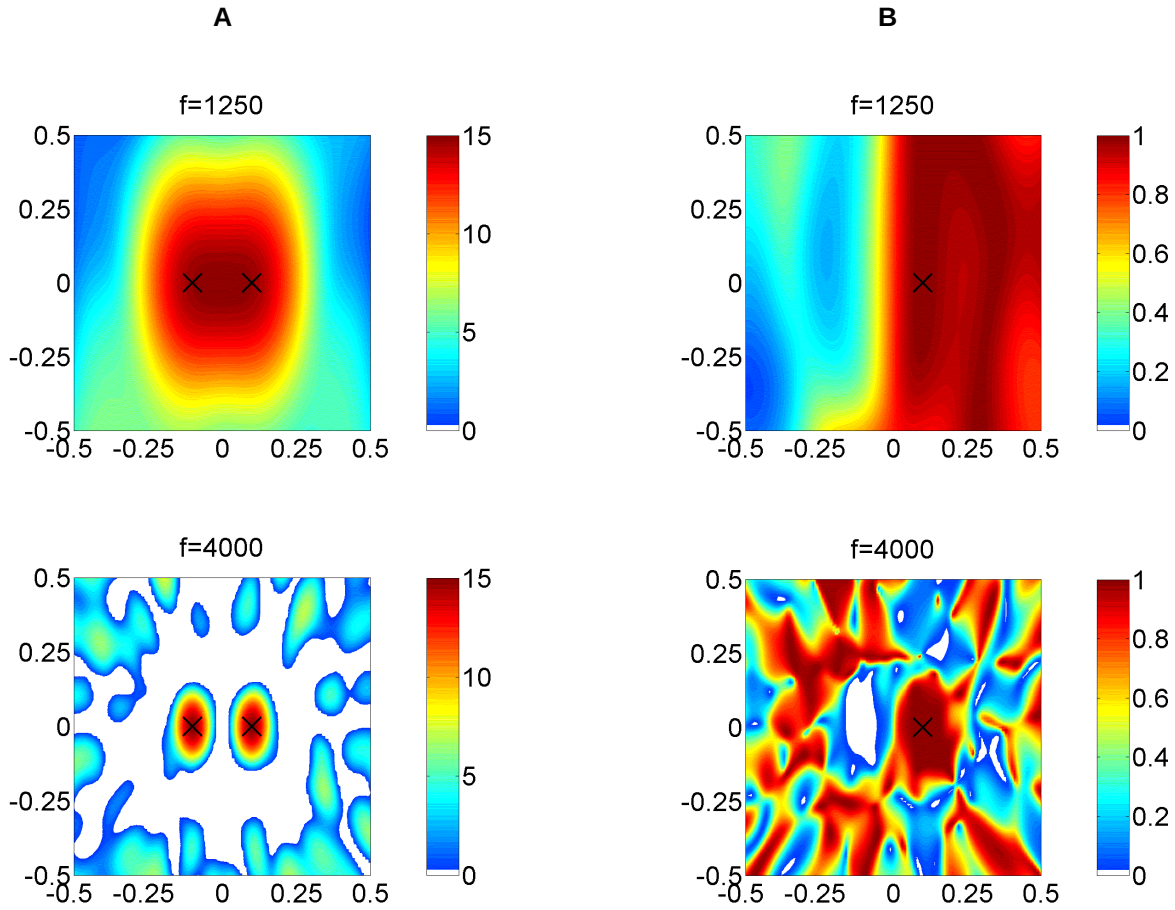

Figure 6: Simulations for two incoherent monopole sources: (A) Acoustic source plots without diagonal-removal processing (1250 and 4000 Hz, source positions indicated by X). (B) Coherence plots with respect to right-hand source (coherence reference point indicated by X).

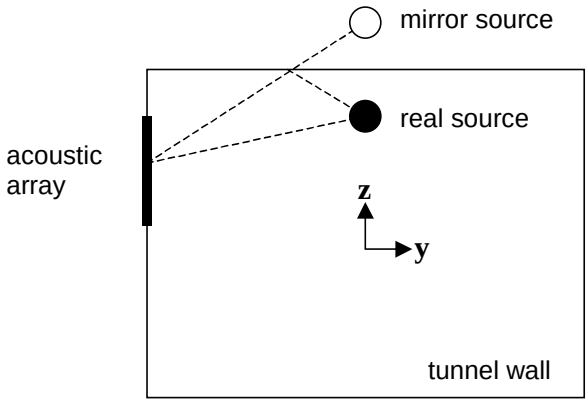

Figure 7: Test set-up for measurements with a calibration source in the closed test section of the DNW-Low Speed Wind Tunnel.

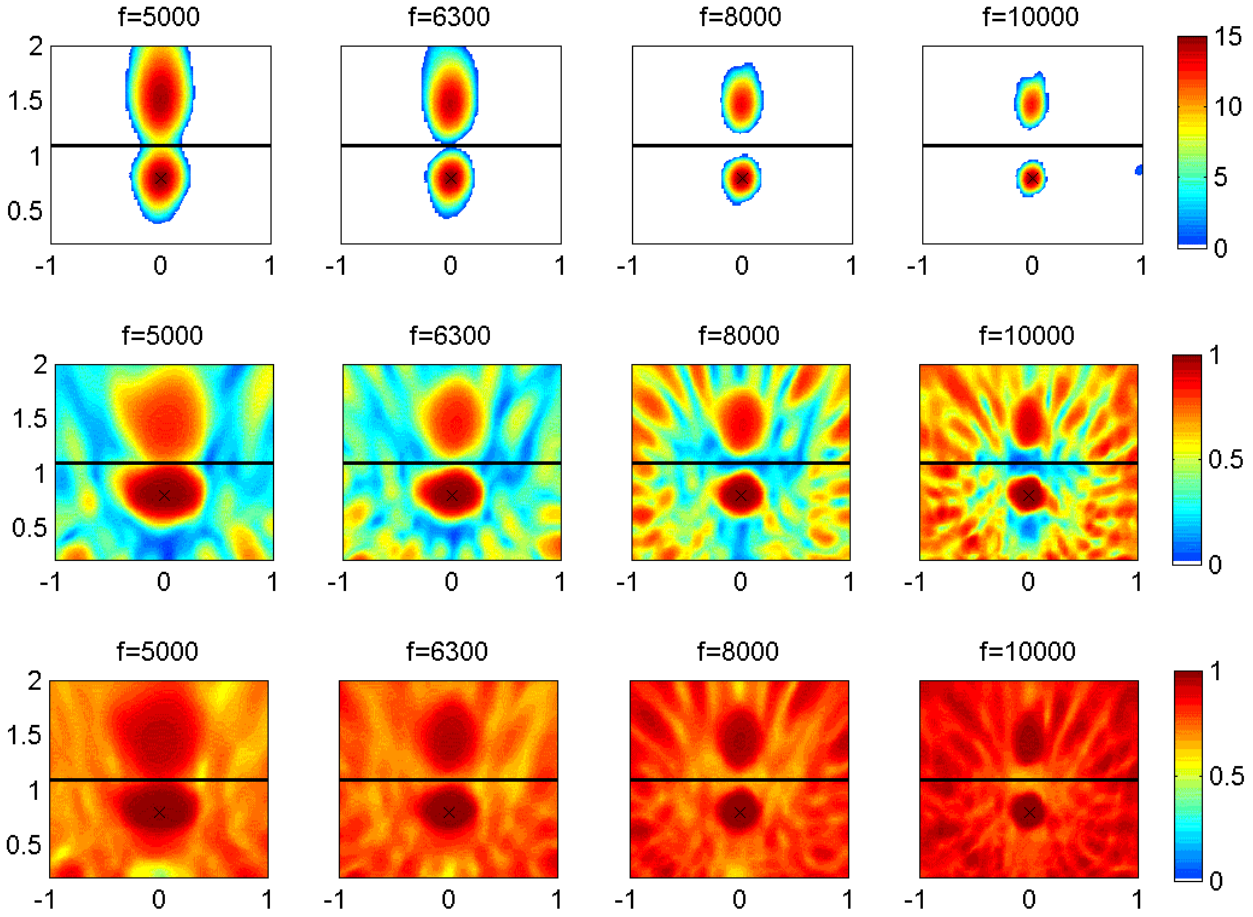

Figure 8: Phased array measurements of calibration source in the closed test section of the DNW-Low Speed Wind Tunnel (no flow), showing real and mirror source. The tunnel ceiling is located at z=1.1 m. (A) Acoustic source plots with diagonal-removal processing (FFT block size is 2048). (B) Coherence plots with respect to real source (block size 2048). (C) Coherence plots for an FFT block size of 8192. The source plots for this case were practically identical to those in A).

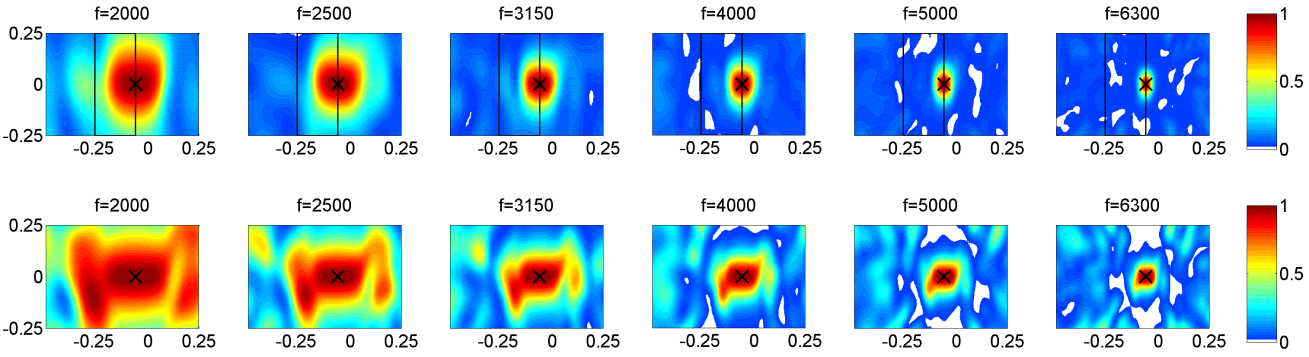

Figure 9: Measured and simulated coherence plots. The coherence reference point is located in the middle of the trailing-edge position. (A) Trailing-edge noise measurements (compare with source plots in Figure 2). (B) Simulations of uncorrelated line source without noise (compare with source plots in Figure 3).

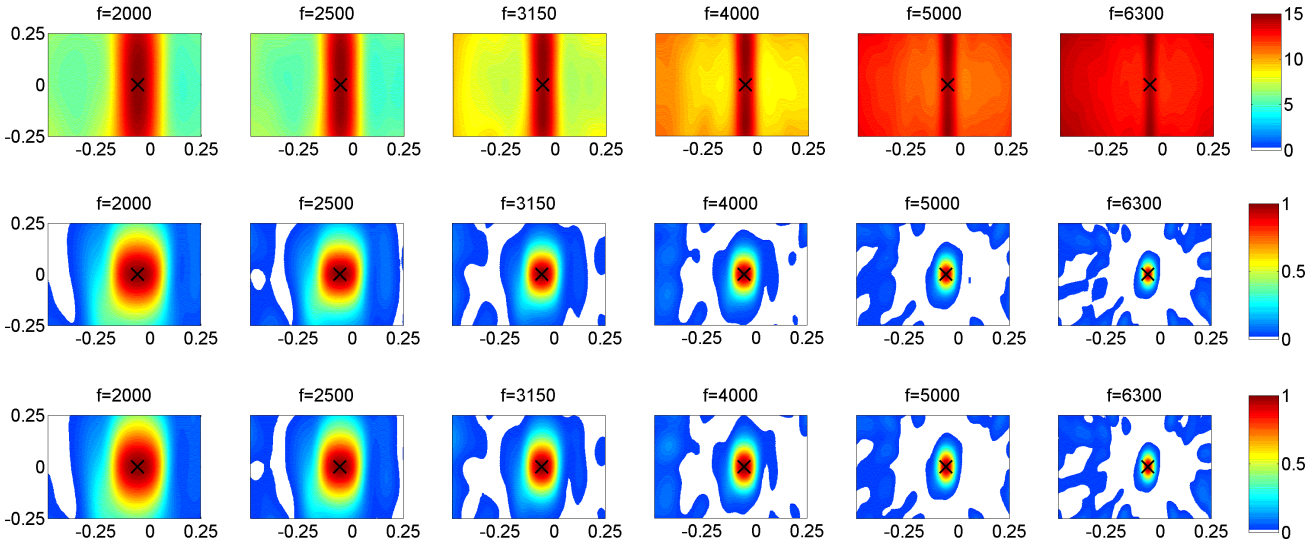

Figure 10: Simulations for line source with noise: (A) Acoustic source plots for uncorrelated line source (without diagonal-removal processing). (B) Coherence plots for uncorrelated line source. (C) Coherence plots for line source with coherence length of 15 cm.

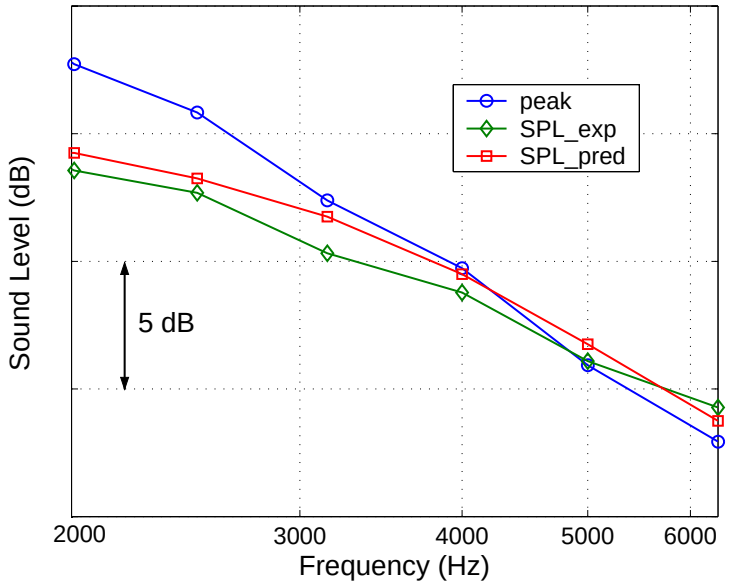

Figure 11: Comparison of trailing-edge noise spectra from measurement and prediction: peak level in measured acoustic source plot ('peak'), experimental trailing-edge noise spectrum using ACF ('SPL_exp'), and predicted trailing-edge noise spectrum (SPL_pred).